

# Pathways for abiotic organic synthesis at submarine hydrothermal fields

Jill M. McDermott<sup>a,1,2</sup>, Jeffrey S. Seewald<sup>a</sup>, Christopher R. German<sup>b</sup>, and Sean P. Sylva<sup>a</sup>

<sup>a</sup>Department of Marine Chemistry and Geochemistry, Woods Hole Oceanographic Institution, Woods Hole, MA 02543; and <sup>b</sup>Department of Geology and Geophysics, Woods Hole Oceanographic Institution, Woods Hole, MA 02543

Edited by Donald E. Canfield, Institute of Biology and Nordic Center for Earth Evolution, University of Southern Denmark, Odense, Denmark, and approved May 11, 2015 (received for review March 30, 2015)

**Arguments for an abiotic origin of low-molecular weight organic compounds in deep-sea hot springs are compelling owing to implications for the sustenance of deep biosphere microbial communities and their potential role in the origin of life. Theory predicts that warm H<sub>2</sub>-rich fluids, like those emanating from serpentinizing hydrothermal systems, create a favorable thermodynamic drive for the abiotic generation of organic compounds from inorganic precursors. Here, we constrain two distinct reaction pathways for abiotic organic synthesis in the natural environment at the Von Damm hydrothermal field and delineate spatially where inorganic carbon is converted into bioavailable reduced carbon. We reveal that carbon transformation reactions in a single system can progress over hours, days, and up to thousands of years. Previous studies have suggested that CH<sub>4</sub> and higher hydrocarbons in ultramafic hydrothermal systems were dependent on H<sub>2</sub> generation during active serpentinization. Rather, our results indicate that CH<sub>4</sub> found in vent fluids is formed in H<sub>2</sub>-rich fluid inclusions, and higher *n*-alkanes may likely be derived from the same source. This finding implies that, in contrast with current paradigms, these compounds may form independently of actively circulating serpentinizing fluids in ultramafic-influenced systems. Conversely, widespread production of formate by  $\Sigma\text{CO}_2$  reduction at Von Damm occurs rapidly during shallow subsurface mixing of the same fluids, which may support anaerobic methanogenesis. Our finding of abiogenic formate in deep-sea hot springs has significant implications for microbial life strategies in the present-day deep biosphere as well as early life on Earth and beyond.**

abiotic organic synthesis | hydrothermal systems | methane | formate | fluid-vapor inclusions

Seawater-derived hydrothermal fluids venting at oceanic spreading centers are a net source for dissolved carbon to the deep sea, with vent fluid carbon contents directly tied to the sustenance of the seafloor biosphere (1). Highly reducing fluids rich in dissolved H<sub>2</sub>, such as those discharging from serpentinizing hydrothermal systems, are of particular interest because of the potential for abiotic reduction of dissolved inorganic carbon ( $\Sigma\text{CO}_2 = \text{CO}_2 + \text{HCO}_3^- + \text{CO}_3^{2-}$ ) to organic compounds (2–6) and their potential role as precursor compounds for prebiotic chemistry associated with the origin of life (7). Although there is increasing evidence that supports an abiotic origin for CH<sub>4</sub> and other low-molecular weight organic compounds in ultramafic-hosted hydrothermal systems (8–10), the physical conditions, reaction pathways, and timescales that control abiotic organic synthesis at oceanic spreading centers remain elusive. Working models for the formation of abiotic CH<sub>4</sub> and other hydrocarbons observed in vent fluids involve reduction of  $\Sigma\text{CO}_2$  and/or CO through Fischer–Tropsch-type processes during active circulation of seawater-derived hydrothermal fluids that are highly enriched in dissolved H<sub>2</sub> because of serpentinization of host rocks; however, this mechanism has not been conclusively shown in natural systems. Others have suggested that leaching of CH<sub>4</sub> and low-molecular weight hydrocarbons from magmatic fluid inclusions hosted in plutonic rocks may contribute at some level to the inventory of organic compounds observed

in axial hot-spring fluids (1, 11, 12). The relative influence of these processes has important implications for the total flux and real-time concentrations of aqueous organic compounds delivered to the oceans by ridge-crest hydrothermal activity. Here, we use multiple lines of evidence to preclude abiotic reduction of  $\Sigma\text{CO}_2$  to CH<sub>4</sub> during active fluid circulation but show that it is reduced to the metastable intermediate species formate instead.

## Results and Discussion

Located at 2,350-m depth on the Mid-Cayman Rise (13, 14), hydrothermal fluids emanate from the Von Damm vent field at temperatures as high as 226 °C (Fig. S1). Ultramafic, gabbroic, and basaltic rocks are associated with the Mount Dent oceanic core complex that hosts this site (15–17). The highest temperature fluids venting at East Summit are characterized by high-dissolved H<sub>2</sub> (18.2 mmol/L), CH<sub>4</sub> (2.81 mmol/L), elevated C<sub>2+</sub> hydrocarbons, low-dissolved metals, near-neutral pH (5.6), and near-zero concentrations of dissolved Mg (Fig. 1A, Table 1, and Fig. S2 A–C). Relative to seawater, dissolved Cl and  $\Sigma\text{CO}_2$  abundances in the near-endmember East Summit fluids are slightly enriched, with concentrations of 651 and 2.80 mmol/kg, respectively (SI Text, section 1). Lower temperature fluids that contain substantial concentrations of Mg are also observed at the summit and around the flanks of the Von Damm mound. Aqueous concentrations of Cl, CH<sub>4</sub>, ethane (C<sub>2</sub>H<sub>6</sub>), and propane

## Significance

**Arguments for an abiotic origin of organic compounds in deep-sea hot springs are compelling because of their potential role in the origin of life and sustaining microbial communities. Theory predicts that warm H<sub>2</sub>-rich fluids circulating through serpentinizing systems create a favorable thermodynamic drive for inorganic carbon reduction to organic compounds. We show that abiotic synthesis proceeds by two spatially and temporally distinct mechanisms. Abundant dissolved CH<sub>4</sub> and higher hydrocarbons are likely formed in H<sub>2</sub>-rich fluid inclusions over geologic timescales. Conversely, formate production by  $\Sigma\text{CO}_2$  reduction occurs rapidly during subsurface mixing, which may support anaerobic methanogenesis. We confirm models for abiotic metastable organic compound formation and argue that alkanes in all ultramafic-influenced vents may form independently of actively circulating serpentinizing fluids.**

Author contributions: J.M.M., J.S.S., and C.R.G. designed research; J.M.M., J.S.S., C.R.G., and S.P.S. performed research; J.M.M., J.S.S., and C.R.G. analyzed data; and J.M.M., J.S.S., and C.R.G. wrote the paper.

The authors declare no conflict of interest.

This article is a PNAS Direct Submission.

Freely available online through the PNAS open access option.

<sup>1</sup>To whom correspondence should be addressed. Email: jillmcdermott@alum.mit.edu.

<sup>2</sup>Present address: Department of Earth Sciences, University of Toronto, Toronto, ON, Canada M5S 3B1.

This article contains supporting information online at [www.pnas.org/lookup/suppl/doi:10.1073/pnas.1506295112/-DCSupplemental](http://www.pnas.org/lookup/suppl/doi:10.1073/pnas.1506295112/-DCSupplemental).

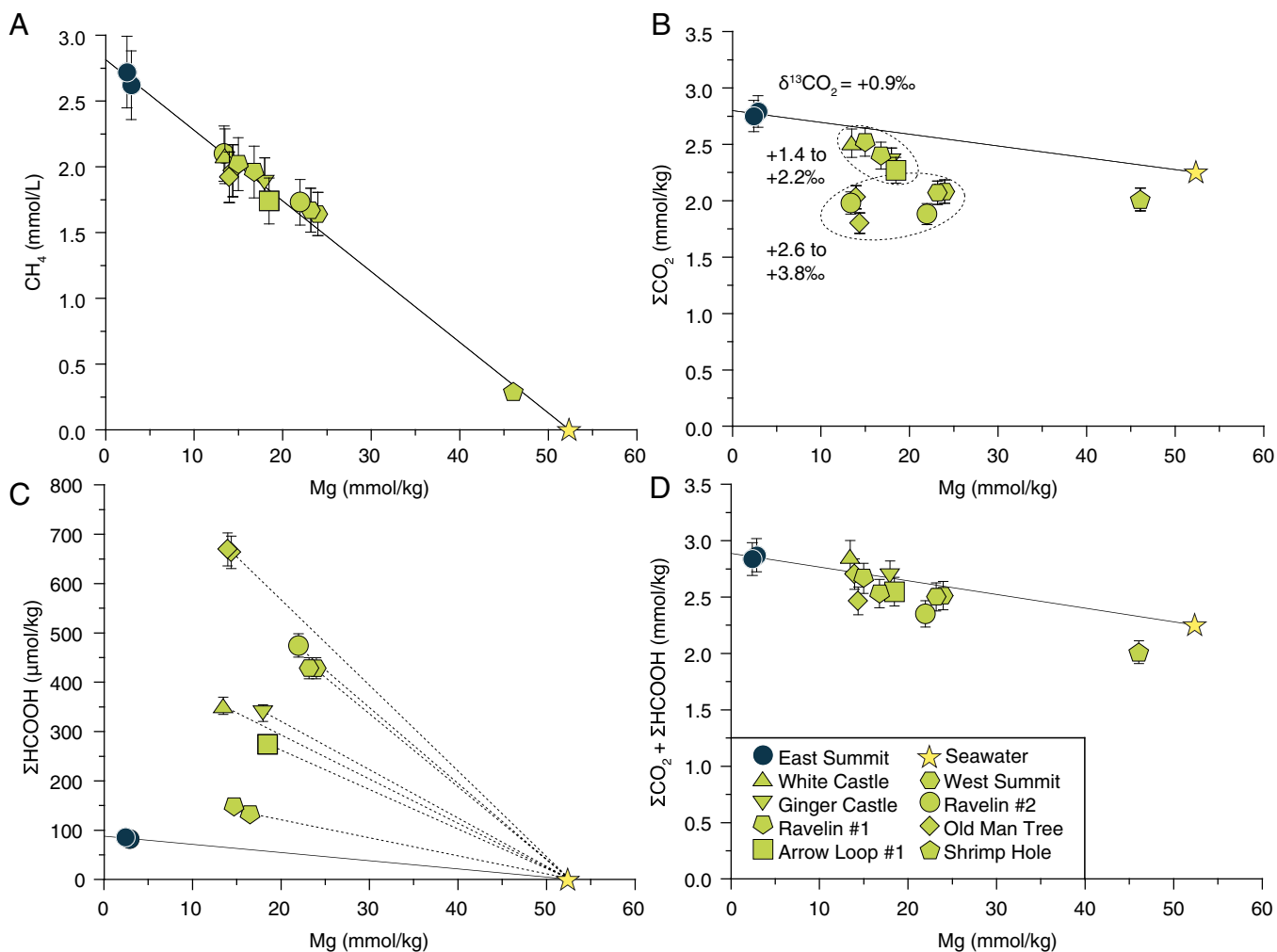


**Fig. 1.** Plots of measured Mg vs. (A)  $\text{CH}_4$ , (B)  $\Sigma\text{CO}_2$ , (C)  $\Sigma\text{HCOOH}$ , and (D)  $\Sigma\text{CO}_2 + \Sigma\text{HCOOH}$  concentrations for Von Damm vent fluids. Mg content is used as an indicator for seawater mixing; solid lines denote conservative dilution of the near-endmember composition (blue circles) with seawater (yellow stars), whereas dashed lines indicate species concentrations that result from nonconservative mixing in elevated Mg fluids (green symbols). Select  $\delta^{13}\text{C}_{\text{CO}_2}$  values are plotted in *B* near corresponding samples. Uncertainties ( $2\sigma$ ) not shown are smaller than symbols.

( $\text{C}_3\text{H}_8$ ) in these fluids define single conservative mixing lines when each species is plotted against dissolved Mg, suggesting that these fluids have formed by subsurface mixing of cold Mg-rich ambient seawater with the same near-zero Mg fluids (18) sampled at the East Summit (Fig. 1*A* and Fig. S2*B–D*).

Elevated concentrations of dissolved  $\text{H}_2$ ,  $\text{CH}_4$ , and low-molecular weight hydrocarbons are remarkably similar to abundances in other ultramafic-influenced hydrothermal systems (8–10, 19), consistent with a strong influence of serpentinization reactions in subsurface reaction zones on the composition of Von Damm vent fluids. The carbon isotopic composition of dissolved  $\text{CH}_4$  is uniform across the Von Damm vent field, with a  $\delta^{13}\text{C}$  value of  $-15.4\text{‰}$  (Table 1). This value is significantly heavier than those typically associated with thermogenic  $\text{CH}_4$  generation ( $-25\text{‰}$  to  $-50\text{‰}$ ) or microbial production of  $\text{CH}_4$  from  $\Sigma\text{CO}_2$  ( $-30\text{‰}$  to  $-70\text{‰}$ ) (20, 21), providing compelling evidence for an abiotic origin for Von Damm  $\text{CH}_4$ . An abiotic origin for  $\text{CH}_4$  has been invoked for other ultramafic-influenced systems at Rainbow, Logatchev, and Lost City hydrothermal fields, where  $\delta^{13}\text{C}$  values for  $\text{CH}_4$  range from  $-9\text{‰}$  to  $-16\text{‰}$  (8–10, 19).

The abundance and isotopic composition of aqueous carbon species in the Von Damm endmember fluids place important constraints on deep-seated processes responsible for the production of  $\text{CH}_4$ . Maximum fluid temperatures at Von Damm are

at least  $150\text{ °C}$  cooler than the predicted two-phase boundary for seawater at in situ seafloor pressures (22), suggesting that the minor Cl enrichment is not the result of subsurface phase separation (Fig. S3). Instead, the 19% enrichment in Von Damm endmember fluid Cl content (Fig. S2*D*) likely reflects the removal of water from seawater-derived fluids during serpentinization hydration reactions at low fluid to rock mass ratio (23). Applying a 19% correction to local bottom seawater  $\Sigma\text{CO}_2$  concentrations ( $2.25 \pm 0.11\text{ mmol/kg}$ ) yields a predicted fluid  $\Sigma\text{CO}_2$  abundance of  $2.69\text{ mmol/kg}$  that matches, within analytical error, the observed endmember  $\Sigma\text{CO}_2$  ( $2.80 \pm 0.14\text{ mmol/kg}$ ). Because the corrected  $\Sigma\text{CO}_2$  abundance of the endmember fluid is nearly identical to that of ambient bottom seawater, we infer that no significant amounts of  $\Sigma\text{CO}_2$  are added to or removed from the fluids during deep convective circulation before mixing in near-seafloor upflow zones. This argument is further supported by the  $\delta^{13}\text{C}$  isotopic composition of the endmember  $\Sigma\text{CO}_2$  ( $0.9\text{‰} \pm 0.3\text{‰}$ ), which is identical, within error, to that of local bottom seawater ( $1.1\text{‰} \pm 0.3\text{‰}$ ). This conservation of  $\Sigma\text{CO}_2$  during circulation through the crust has profound implications for the origin of the  $\text{CH}_4$  in Von Damm vent fluids. With the addition of  $2.81\text{ mmol/kg}$   $\text{CH}_4$ , the endmember fluids contain approximately double the total carbon content of ambient seawater. Because the  $\Sigma\text{CO}_2$  in the endmember fluids cannot provide the source of this carbon, this

**Table 1. Measured and calculated abundance and stable isotope data for Von Damm vent fluids**

Vent	Sample	T (°C)	Mg (mm)	pH*	Cl (mm)	H <sub>2</sub> (mM)	ΣHCOOH (μm)	ΣCO <sub>2</sub> (mm)	CH <sub>4</sub> (mM)	C <sub>2</sub> H <sub>6</sub> (nm)	C <sub>3</sub> H <sub>8</sub> (nm)	δ <sup>13</sup> C <sub>CO2</sub> (‰)	δ <sup>13</sup> C <sub>CH4</sub> (‰)	δ <sup>13</sup> C <sub>C2H6</sub> (‰)	δ <sup>13</sup> C <sub>C3H8</sub> (‰)
East Summit	Endmember	—	0	5.56	651	18.2	88.2	2.80	2.81	639	56	NA	NA	NA	NA
East Summit	J2-612-IGT2	226	2.93	5.65	649	16.2	82.0	2.79	2.62	603	52	0.8	-15.6	-12.9	-9.8
East Summit	J2-616-IGT8	226	2.43	5.56	641	18.3	85.6	2.75	2.72	—	—	0.9	-15.3	-12.3	—
White Castle	J2-616-IGT1	151	13.5	5.77	622	13.1	352 <sup>†</sup>	2.51	2.08	485	41	1.5	-15.6	—	—
Ginger Castle	J2-617-IGT4	125	18.0	6.06	604	11.3	337 <sup>†</sup>	2.35	1.88	—	—	2.2	-15.8	-13.2	-10.8
Ravelin 1	J2-617-IGT6	145	15.0	5.83	614	13.4	147 <sup>†</sup>	2.52	2.02	—	—	1.9	-15.6	—	—
Ravelin 1	J2-617-IGT2	131	16.8	5.93	616	13.1	132	2.40	1.96	431	38	1.4	-15.1	—	—
Arrow Loop 1	J2-616-IGT6	134	18.5	5.86	616	10.8	274 <sup>†</sup>	2.27	1.74	417	36	1.9	-15.7	-12.5	—
West Summit	J2-621-IGT1	123	24.0	6.00	605	9.94	428	2.08	1.64	359	30	3.3	-15.6	-12.6	—
West Summit	J2-621-IGT4	123	23.2	6.01	597	9.94	428 <sup>†</sup>	2.07	1.67	335	29	3.6	-15.1	—	—
Ravelin 2	J2-621-IGT2	116	13.4	5.88	620	13.6	—	1.98	2.10	475	40	3.8	-15.1	-12.9	-9.7
Ravelin 2	J2-621-IGT8	115	22.0	6.12	600	10.9	474 <sup>†</sup>	1.88	1.73	365	34	3.3	-15.4	-12.7	—
Old Man Tree	J2-612-IGT6	115	14.4	5.81	620	10.5	663	1.80	1.97	—	—	2.6	-15.2	—	—
Old Man Tree	J2-612-IGT8	114	14.0	5.89	621	10.2	669 <sup>†</sup>	2.03	1.92	455	40	2.9	-15.0	-12.6	-11.6
Shrimp Hole	J2-617-IGT1	21	46.1	7.73	549	0.01	BD	2.01	0.29	51.8	4.6	1.1	-15.1	—	—
Bottom SW		~5	52.4	~8	545	0	~1	2.25	0	0	0	1.1	NA	NA	NA

Analytical uncertainties (2σ) are ±2 °C for T; ±3% for Mg and Cl; ±5% for H<sub>2</sub>, ΣHCOOH, ΣCO<sub>2</sub>, CH<sub>4</sub>, C<sub>2</sub>H<sub>6</sub>, and C<sub>3</sub>H<sub>8</sub>; ±0.05 units for pH; ±0.3% for δ<sup>13</sup>C<sub>CO2</sub>; ±0.8‰ for δ<sup>13</sup>C<sub>CH4</sub>; ±0.4‰ for δ<sup>13</sup>C<sub>C2H6</sub>; and ±0.7‰ for δ<sup>13</sup>C<sub>C3H8</sub>. Values that were not determined are indicated by —. BD, below detection (1.0 μm for ΣHCOOH); IGT, isobaric gas tight; mm, mmol/kg; mM, mmol/L; μm, μmol/kg; NA, not applicable; nm, nmol/kg; SW, seawater; T, temperature.

\*Shipboard pH is reported (25 °C and 1 atm).

<sup>†</sup>Sample used to calculate measured affinities in Fig. 2.

finding implies that CH<sub>4</sub> formation from reduction of inorganic sources is not occurring during active fluid circulation at the Von Damm site. Because CH<sub>4</sub> is the dominant product expected during abiogenic *n*-alkane synthesis (11), we infer that C<sub>2+</sub> hydrocarbon formation is also not occurring during active fluid circulation.

Radiocarbon analysis provides additional confirmation that Von Damm CH<sub>4</sub> is not derived from fluid ΣCO<sub>2</sub> contents. The four Von Damm CH<sub>4</sub> samples measured, including the East Summit fluid, all reveal <sup>14</sup>C contents near the detectable limit [fraction modern (*F<sub>m</sub>*) = 0.0025] (Table S1). In contrast, corresponding ΣCO<sub>2</sub> samples contain detectable modern <sup>14</sup>C contents (*F<sub>m</sub>* = 0.0236–0.0373) that would be transferred to CH<sub>4</sub> if it were generated by ΣCO<sub>2</sub> reduction occurring during fluid circulation (Table S1). Thus, the model postulated for the formation of abundant CH<sub>4</sub> at the Lost City vent field involving the leaching of radiocarbon-dead ΣCO<sub>2</sub> from fluid inclusions hosted in plutonic rocks and its subsequent reduction to CH<sub>4</sub> during hydrothermal fluid circulation (8) cannot account for the occurrence of CH<sub>4</sub> at Von Damm.

In contrast, we suggest that CH<sub>4</sub> and C<sub>2+</sub> hydrocarbons in the Von Damm vent fluids are derived from leaching of carbon-rich fluid inclusions at depth. We postulate that the abundant CH<sub>4</sub>, C<sub>2</sub>H<sub>6</sub>, and C<sub>3</sub>H<sub>8</sub> in Von Damm vent fluids were formed when magmatic volatiles trapped in plutonic rocks reequilibrated during cooling to temperatures <400 °C, generating hydrocarbon-rich and ΣCO<sub>2</sub>-poor fluid–vapor inclusions as described for CH<sub>4</sub>-rich Southwest Indian Ridge gabbros (12, 24). We propose that, at Von Damm, these hydrocarbons are subsequently liberated during hydrothermal alteration of the Mount Dent oceanic core complex host rocks (15–17). CH<sub>4</sub> observed in Southwest Indian Ridge plutonic rock fluid inclusions is characterized by δ<sup>13</sup>C values of -10‰ to -30‰ (1, 25), a range that matches the values for not just the Von Damm field (-15.4‰) but also, all previously studied ultramafic-influenced submarine hydrothermal fields (8–10). This observation, again, supports our arguments that the processes that we reveal here may be directly relevant to all such systems.

Another line of evidence supporting a magmatic volatile-rich fluid inclusion input is the isotopic composition of He in the Von

Damm vent fluids, which indicates *R/R<sub>a</sub>* values of 8.0–8.2 that are consistent with a mantle source (26) (Table S2). Measured CH<sub>4</sub><sup>3</sup>He ratios (~2.4 × 10<sup>8</sup>) that are just below the average value of ΣCO<sub>2</sub><sup>3</sup>He measured in mantle rocks (1 × 10<sup>9</sup>) (26) also support a mantle-derived (fluid inclusion) source for the hydrocarbons. This CH<sub>4</sub><sup>3</sup>He ratio suggests a conversion of ~24% of mantle-derived carbon to CH<sub>4</sub>. Formation of graphite, which can precipitate on cooling of plutonic fluid inclusions (12), may account for the remainder of the carbon.

Thermodynamic models for the abiotic synthesis of aqueous organic compounds under hydrothermal conditions have postulated that kinetic barriers to the formation of CH<sub>4</sub> preclude stable equilibrium in the C-H-O chemical system, thereby creating a thermodynamic drive for the formation of metastable organic species in submarine hot springs (3, 4). The abundance of aqueous carbon species more oxidized than CH<sub>4</sub> in Von Damm vent fluids supports such a model. For example, in contrast to dissolved CH<sub>4</sub> concentrations, concentrations of ΣCO<sub>2</sub> in lower temperature mixed fluids at Von Damm are depleted by as much as 25% relative to a conservative mixing assumption. These depletions are accompanied by <sup>13</sup>C enrichment of the residual ΣCO<sub>2</sub> compared with the endmember vent fluids and seawater (Fig. 1B and Table 1) and significantly enriched formate species (ΣHCOOH = HCOOH + HCOO<sup>-</sup>) abundances of 73–605 μmol/kg relative to conservative mixing (Fig. 1C). This result suggests that abiotic ΣHCOOH formation represents a sink for vent fluid ΣCO<sub>2</sub> in subsurface mixing zones. Consistent with this interpretation, the amount of carbon present as ΣHCOOH and ΣCO<sub>2</sub> in the endmember fluid at East Summit remains constant during mixing in the cooler fluids (Fig. 1D). Despite a strong thermodynamic drive, CH<sub>4</sub> production from ΣCO<sub>2</sub> does not occur because of well-established kinetic limitations, permitting the formation of metastable intermediate ΣHCOOH species. Reduction of ΣCO<sub>2</sub> by H<sub>2</sub> in mixed fluids (CO<sub>2</sub> + H<sub>2</sub> = HCOOH) is consistent with thermodynamic predictions in the absence of CH<sub>4</sub> production and laboratory experiments that have shown rapid reaction kinetics over hour to day timescales (2, 6) and isotopic enrichment of the residual ΣCO<sub>2</sub>.



**Thermodynamic Evaluation of  $\Sigma\text{HCOOH}$  Abundances.** Fluid compositions are consistent with metastable thermodynamic equilibrium between  $\Sigma\text{CO}_2$ ,  $\Sigma\text{HCOOH}$ , and  $\text{H}_2$  in Von Damm mixed fluids, providing additional support for an abiotic origin. Formation of  $\Sigma\text{HCOOH}$  on mixing represents a move to a near-equilibrium condition as indicated by decreasing chemical affinities that reach values below 5 kJ/mol for most of the sampled fluids (Fig. 2 and *SI Text*, section 2). Thus, unlike  $\text{CH}_4$ , the absence of kinetic barriers allows for abiotic synthesis of  $\Sigma\text{HCOOH}$  in subsurface mixing zones during active circulation of submarine hydrothermal fluids.

Because of kinetic inhibition of  $\text{CH}_4$  formation, there is a thermodynamic drive for the abiotic production of other metastable low-molecular weight organic species in addition to  $\Sigma\text{HCOOH}$ . Although methanol ( $\text{CH}_3\text{OH}$ ) production from  $\Sigma\text{CO}_2$  and  $\text{H}_2$  is thermodynamically favorable at Von Damm, the predicted metastable equilibrium  $\text{CH}_3\text{OH}$  abundances in mixed fluids would be greater than predicted  $\Sigma\text{CO}_2$  abundances, exceeding 2 mmol/kg. Our observation that the amounts of carbon present as  $\Sigma\text{HCOOH}$  and  $\Sigma\text{CO}_2$  remain constant during mixing (Fig. 1D), therefore, precludes equilibrium  $\text{CH}_3\text{OH}$  formation. Similarly, abiotic production of other carboxylic acids (e.g., acetic, propanoic, and butanoic) is likely kinetically inhibited, because these species are below detection ( $< 1 \mu\text{mol/kg}$ ). The organosulfur compound methanethiol ( $\text{CH}_3\text{SH}$ ) is present in Von Damm fluids at abundances that do not reflect metastable equilibrium with  $\Sigma\text{CO}_2$  and has been attributed to thermal alteration of microbial biomass or other sources of preexisting organic matter (27). The presence of other potential metastable species, such as amino acids, was not investigated; however, if they formed on mixing, it is likely that their concentrations are below the precision of  $\Sigma\text{CO}_2$  analysis ( $\sim 100 \mu\text{mol/kg}$ ).

**Implications.** Vent microorganisms inhabit environments dominated by mixed hydrothermal fluids, where  $\Sigma\text{HCOOH}$  can be used as an energy or fixed carbon source by methanogenesis. With abundances approaching those of  $\Sigma\text{CO}_2$ ,  $\Sigma\text{HCOOH}$ -based methanogenesis could be a viable metabolic strategy at Von Damm, and abiotic  $\Sigma\text{HCOOH}$  may represent an important substrate for microorganisms in high- $\text{H}_2$  hydrothermal fluids, which

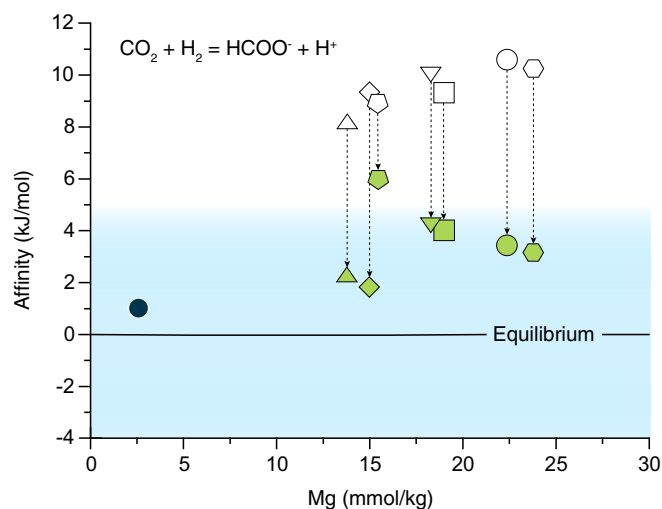


**Fig. 2.** Chemical affinity for the production of  $\text{HCOO}^-$  from  $\Sigma\text{CO}_2$  and  $\text{H}_2$  in Von Damm mixed fluids. White symbols indicate a thermodynamic drive for reaction (positive affinity) as written based on conservative dilution of the near-endmember  $\Sigma\text{HCOOH}$  composition (blue circle). Green symbols denote affinity calculated with actual mixed fluid  $\Sigma\text{HCOOH}$  contents. Thermodynamic equilibrium is defined as affinity =  $0 \pm 5$  kJ/mol (light blue shading). Symbol shapes correspond to those in Fig. 1.

was hypothesized previously for Lost City (28, 29). Formate is the first intermediate species formed in the acetyl-CoA pathway (30), and its abiotic production can reduce the energetic demand for an organism, while also serving as the first step toward forming reduced carbon species that were central to primitive biochemical pathways on early Earth (31). Our demonstration of abiotic production of  $\text{CH}_4$  and likely,  $\text{C}_{2+}$  *n*-alkanes in deep-sea hydrothermal systems is also relevant to understanding metabolic options on early Earth environments as well as life strategies in modern systems.

Fluid circulation at Von Damm integrates abiotic organic species formed on long as well as short timescales. Hydrothermal fluids are rich in  $\text{CH}_4$  leached from ancient magmatic volatile fluid inclusions hosted in plutonic rocks, where it is formed over geologic timescales, and  $\Sigma\text{HCOOH}$ , which is formed actively during shallow subsurface mixing over hours to days. These findings represent a fundamental advance in our understanding of processes leading to abiotic organic synthesis in modern and ancient systems on Earth as well as other planetary bodies (7, 31, 32). Furthermore, the demonstration of ongoing  $\Sigma\text{HCOOH}$  synthesis is important for microbial communities in the present-day oceanic crust, with exciting implications for microbial metabolisms and life strategies in any warm high- $\text{H}_2$  natural waters.

## Materials and Methods

Vent fluid samples were collected using 150-mL titanium isobaric gas-tight samplers (33) deployed by the remotely operated vehicle *Jason II* aboard the *R/V Atlantis* (Cruise AT18-16) in January of 2012. Thermocouples were calibrated with a National Institute of Standards and Technology temperature calibrator, and the maximum measured temperature for each sample is reported (Table 1). Samples were extracted and processed within 24 h of sampler recovery. Immediately after withdrawing the fluid aliquot from the isobaric gas-tight sampler, pH (25 °C and 1 atm) was measured by potentiometry using an Ag/AgCl reference electrode. Aliquots were collected in Optima HCl-cleaned high-density polyethylene bottles for shore-based analysis of Mg, Cl, and total formate species ( $\Sigma\text{HCOOH} = \text{HCOOH} + \text{HCOO}^-$ ) in samples stored frozen. Shipboard measurement of dissolved  $\text{H}_2$  and  $\text{CH}_4$  was accomplished by molecular-sieve gas chromatography (GC) with thermal conductivity detection after a headspace extraction (3, 34). Aliquots for shore-based total dissolved inorganic carbon ( $\Sigma\text{CO}_2 = \text{CO}_3^{2-} + \text{HCO}_3^- + \text{H}_2\text{CO}_3$ ) abundance and stable and radiocarbon isotope analysis of  $\text{CH}_4$  and  $\Sigma\text{CO}_2$  were transferred to evacuated 25-mL serum vials poisoned with  $\text{Hg}_2\text{Cl}$  and sealed with butyl rubber stoppers that were preboiled in NaOH to remove trace hydrocarbons (35). Dissolved He was extracted from fluid samples on board the ship using a portable vacuum line and transferred to evacuated aluminosilicate glass break-seal tubes for shore-based He isotope analysis. Fluid aliquots were transferred into sealed glass tubes fitted with Teflon and stainless steel valves for shore-based  $\text{C}_2\text{H}_6$  and  $\text{C}_3\text{H}_8$  analysis using a purge and trap device interfaced to molecular-sieve GC with flame ionization detection (34). Dissolved Cl and  $\Sigma\text{HCOOH}$  abundances were determined by ion chromatography (36, 37). Dissolved Mg concentrations were determined on a Thermo-Electron Element2 inductively coupled plasma mass spectrometer (MS) (36, 38). Dissolved  $\Sigma\text{CO}_2$  abundances were determined by headspace gas GC injection with thermal conductivity detection (34, 36). Stable carbon isotopes ( $\delta^{13}\text{C}_{\Sigma\text{CO}_2}$  and  $\delta^{13}\text{C}_{\text{CH}_4}$ ) were measured by isotope ratio monitoring MS using a Finnigan DeltaPlusXL Mass Spectrometer coupled to an Agilent 6890 GC (1,150 °C combustion temperature). Stable carbon isotope data are reported in standard  $\delta$ -notation ( $\delta^{13}\text{C}$ ) expressed as

$$\delta^{13}\text{C}(\text{‰}) = \left[ \frac{R_{\text{samp}} - R_{\text{std}}}{R_{\text{std}}} \right] \times 1,000, \quad [1]$$

where  $R_{\text{samp}}$  and  $R_{\text{std}}$  are the isotope ratios ( $^{13}\text{C}/^{12}\text{C}$ ) of the sample and the standard, respectively. Carbon stable isotopes are reported relative to the Vienna Pee Dee Belemnite Scale. Because of variable entrainment of ambient seawater that contains 2.25 mmol/kg  $\text{CO}_2$  with a  $\delta^{13}\text{C}_{\Sigma\text{CO}_2}$  value of 1.1‰, reported sample  $\delta^{13}\text{C}_{\Sigma\text{CO}_2}$  values have been calculated from measured values using isotope mass balance (34). Analytical uncertainties ( $2\sigma$ ) in abundance and isotopic analyses are listed in Table 1. Radiocarbon ( $^{14}\text{C}_{\Sigma\text{CO}_2}$  and  $^{14}\text{C}_{\text{CH}_4}$ ) analysis was conducted at the Woods Hole Oceanographic Institution National Ocean Sciences Accelerator Mass Spectrometry Facility (Table S1). Results are expressed in terms of  $F_{\text{mv}}$  representing the deviation of the sample relative to the modern National Bureau of Standards Oxalic Acid I

standard (NIST-SRM-4990; A.D. 1950) (39). Correction of  $\Sigma\text{CO}_2$  radiocarbon measurements (Table S1) removes the effects of entrainment of ambient seawater through an isotopic mass balance approach that is analogous to the approach for  $\delta^{13}\text{C}_{\Sigma\text{CO}_2}$ . [For example, this calculation uses vent fluid [Mg] as measured, East Summit fluid [ $\Sigma\text{CO}_2$ ] as measured, Ravelin 2 fluid [ $\Sigma\text{CO}_2$ ] assuming conservative endmember-seawater mixing (i.e., before  $\Sigma\text{HCOOH}$  formed), seawater [Mg] = 52.4 mmol/kg, seawater [ $\Sigma\text{CO}_2$ ] = 2.25 mmol/kg, and seawater  $F_m$  = 0.9300 (~580 y, estimated from 2,500-m depth; World Ocean Circulation Experiment Caribbean line A22, 1997).] Measured analytical uncertainties are listed in Table S1. Corrected  $\Sigma\text{CO}_2$  uncertainties are conservative estimates calculated by error propagation of independent variables (e.g., also taking into account the effects of [Mg] and [ $\Sigma\text{CO}_2$ ] analytical uncertainties). He abundance and isotope compositions were determined at

the Isotope Geochemistry Facility at Woods Hole Oceanographic Institution (Table S2). Helium was cryogenically separated from the other noble gases (40), and analyzed as described in the work by German et al. (13). Uncertainties for  $^4\text{He}$  abundances are approximately  $\pm 5\%$  because of splitting procedures (Table S2).

**ACKNOWLEDGMENTS.** We thank the captain and crew of the *R/V Atlantis* and the *ROV Jason II* team for their dedication, expertise, and assistance with sample collection. We also thank M. D. Kurz and J. M. Curtice for the isotopic analysis of helium and J. C. Kinsey for generating the bathymetric map. Financial support for this research was provided by National Aeronautics and Space Administration Award NNX-327 09AB75G, National Science Foundation Award OCE-1061863, and the Woods Hole Oceanographic Institution Ocean Ridge Initiative.

1. Kelley DS, Baross JA, Delaney JR (2002) Volcanoes, fluids, and life at mid-ocean ridge spreading centers. *Annu Rev Earth Planet Sci* 30(1):385–491.
2. Seewald JS, Zolotov M, McCollom TM (2006) Experimental investigation of single carbon compounds under hydrothermal conditions. *Geochim Cosmochim Acta* 70(2):446–460.
3. Shock EL (1990) Geochemical constraints on the origin of organic compounds in hydrothermal systems. *Orig Life Evol Biosph* 20(3-4):331–367.
4. Shock EL (1992) Chemical environments in submarine hydrothermal systems. *Marine Hydrothermal Systems and the Origin of Life*, ed Holm NG (Springer, Dordrecht, The Netherlands), pp 67–107.
5. Shock EL, Schulte MD (1998) Organic synthesis during fluid mixing in hydrothermal systems. *J Geophys Res* 103(E12):28513–28527.
6. McCollom TM (2003) Experimental constraints on the hydrothermal reactivity of organic acids and acid anions: I. Formic acid and formate. *Geochim Cosmochim Acta* 67(19):3625–3644.
7. Martin W, Baross J, Kelley D, Russell MJ (2008) Hydrothermal vents and the origin of life. *Nat Rev Microbiol* 6(11):805–814.
8. Proskurowski G, et al. (2008) Abiogenic hydrocarbon production at lost city hydrothermal field. *Science* 319(5863):604–607.
9. Charlou JL, Donval JP, Fouquet Y, Jean-Baptiste P, Holm NG (2002) Geochemistry of high  $\text{H}_2$  and  $\text{CH}_4$  vent fluids issuing from ultramafic rocks at the Rainbow hydrothermal field (36°14'N, MAR). *Chem Geol* 191(4):345–359.
10. Charlou JL, et al. (2010) High production and fluxes of  $\text{H}_2$  and  $\text{CH}_4$  and evidence of abiotic hydrocarbon synthesis by serpentinization in ultramafic-hosted hydrothermal systems on the Mid-Atlantic Ridge. *Diversity of Hydrothermal Systems on Slow Spreading Ocean Ridges*, eds Rona PA, Devey CW, Dymont J, Murton BJ (American Geophysical Union, Washington, DC), pp 265–296.
11. McCollom TM, Seewald JS (2007) Abiotic synthesis of organic compounds in deep-sea hydrothermal environments. *Chem Rev* 107(2):382–401.
12. Kelley DS, Früh-Green GL (1999) Abiogenic methane in deep-seated mid-ocean ridge environments: Insights from stable isotope analyses. *J Geophys Res* 104(B5):10439–10460.
13. German CR, et al. (2010) Diverse styles of submarine venting on the ultraslow spreading Mid-Cayman Rise. *Proc Natl Acad Sci USA* 107(32):14020–14025.
14. Connelly DP, et al. (2012) Hydrothermal vent fields and chemosynthetic biota on the world's deepest seafloor spreading centre. *Nat Commun* 3:620.
15. Ballard RD, et al. (1979) Geological and geophysical investigation of the Mid-Cayman Rise Spreading Center: Initial results and observations. *Deep Drilling Results in the Atlantic Ocean: Ocean Crust*, eds Talwani M, Harrison CG, Hayes DE (American Geophysical Union, Washington, DC), pp 66–93.
16. Stroup J, Fox P (1981) Geologic investigations in the Cayman Trough: Evidence for thin oceanic crust along the Mid-Cayman Rise. *J Geol* 89(4):395–420.
17. Hayman NW, et al. (2011) Oceanic core complex development at the ultraslow spreading Mid-Cayman Spreading Center. *Geochem Geophys Geosyst*, 10.1029/2010GC003240.
18. Bischoff J, Dickson F (1975) Seawater-basalt interaction at 200°C and 500 bars: Implications for the origin of seafloor heavy metal deposits and regulation of seawater chemistry. *Earth Planet Sci Lett* 25(3):385–397.
19. Schmidt K, Koschinsky A, Garbe-Schönberg D, de Carvalho L, Seifert R (2007) Geochemistry of hydrothermal fluids from the ultramafic-hosted Logatchev hydrothermal field, 15°N on the Mid-Atlantic Ridge: Temporal and spatial investigation. *Chem Geol* 242(1-2):1–21.
20. Valentine DL, Chidthaisong A, Rice A, Reeburgh WS, Tyler SC (2004) Carbon and hydrogen isotope fractionation by moderately thermophilic methanogens. *Geochim Cosmochim Acta* 68(7):1571–1590.
21. Schoell M (1980) The hydrogen and carbon isotopic composition of methane from natural gases of various origins. *Geochim Cosmochim Acta* 44(5):649–661.
22. Bischoff JL, Rosenbauer RJ (1985) An empirical equation of state for hydrothermal seawater (3.2 percent NaCl). *Am J Sci* 285(8):725–763.
23. Allen DE, Seyfried WE, Jr (2004) Serpentinization and heat generation: Constraints from Lost City and Rainbow hydrothermal systems. *Geochim Cosmochim Acta* 68(6):1347–1354.
24. Kelley DS (1996) Methane-rich fluids in the oceanic crust. *J Geophys Res* 101(B2):2943–2962.
25. Kelley DS, Früh-Green GL (2001) Volatile lines of descent in submarine plutonic environments: Insights from stable isotope and fluid inclusion analyses. *Geochim Cosmochim Acta* 65(19):3325–3346.
26. Marty B, Tolstikhin IN (1998)  $\text{CO}_2$  fluxes from mid-ocean ridges, arcs and plumes. *Chem Geol* 145(3-4):233–248.
27. Reeves EP, McDermott JM, Seewald JS (2014) The origin of methanethiol in midocean ridge hydrothermal fluids. *Proc Natl Acad Sci USA* 111(15):5474–5479.
28. Lang SQ, Butterfield DA, Schulte M, Kelley DS, Lilley MD (2010) Elevated concentrations of formate, acetate and dissolved organic carbon found at the Lost City hydrothermal field. *Geochim Cosmochim Acta* 74(3):941–952.
29. Lang SQ, et al. (2012) Microbial utilization of abiogenic carbon and hydrogen in a serpentinite-hosted system. *Geochim Cosmochim Acta* 92(1):82–99.
30. Fuchs G (1986)  $\text{CO}_2$  fixation in acetogenic bacteria: Variations on a theme. *FEMS Microbiol Rev* 39(3):181–213.
31. Martin W, Russell MJ (2007) On the origin of biochemistry at an alkaline hydrothermal vent. *Philos Trans R Soc Lond B Biol Sci* 362(1486):1887–1925.
32. Russell MJ, Hall AJ, Martin W (2010) Serpentinization as a source of energy at the origin of life. *Geobiology* 8(5):355–371.
33. Seewald JS, Doherty K, Hammar T, Liberatore S (2002) A new gas-tight isobaric sampler for hydrothermal fluids. *Deep Sea Res Part 1 Oceanogr Res Pap* 49(1):189–196.
34. Cruse A, Seewald JS (2006) Geochemistry of low-molecular weight hydrocarbons in hydrothermal fluids from Middle Valley, northern Juan de Fuca Ridge. *Geochim Cosmochim Acta* 70(8):2073–2092.
35. Oremland RS, Des Marais DJ (1983) Distribution, abundance and carbon isotopic composition of gaseous hydrocarbons in Big Soda Lake, Nevada: An alkaline, meromictic lake. *Geochim Cosmochim Acta* 47(12):2107–2114.
36. Reeves EP, et al. (2011) Geochemistry of hydrothermal fluids from the PACMANUS, Northeast Pual and Vienna Woods hydrothermal fields, Manus Basin, Papua New Guinea. *Geochim Cosmochim Acta* 75(4):1088–1123.
37. McCollom TM, Seewald JS (2001) A reassessment of the potential for reduction of dissolved  $\text{CO}_2$  to hydrocarbons during serpentinization of olivine. *Geochim Cosmochim Acta* 65(21):3769–3778.
38. Craddock PR, et al. (2010) Rare earth element abundances in hydrothermal fluids from the Manus Basin, Papua New Guinea: Indicators of sub-seafloor hydrothermal processes in back-arc basins. *Geochim Cosmochim Acta* 74(19):5494–5513.
39. Olsson I (1970) The use of oxalic acid as a standard. *Proceedings of the Radiocarbon Variations and Absolute Chronology Nobel Symposium*, ed Olsson I (Wiley, Chichester, United Kingdom), p 17.
40. Lott DE (2001) Improvements in noble gas separation methodology: A nude cryogenic trap. *Geochem Geophys Geosyst*, 10.1029/2001GC000202.
41. Johnson J, Oelkers E, Helgesen H (1992) SUPCRT92: A software package for calculating the standard molal thermodynamic properties of minerals, gases, aqueous species, and reactions from 1 to 5000 bar and 0 to 1000°C. *Comput Geosci* 18(7):899–947.
42. Shock EL (1995) Organic acids in hydrothermal solutions: Standard molal thermodynamic properties of carboxylic acids and estimates of dissociation constants at high temperatures and pressures. *Am J Sci* 295(5):496–580.
43. Wolery TJ (1992) *EQ3NR, A Computer Program for Geochemical Aqueous Speciation-Solubility Calculations: Theoretical Manual, User's Guide, and Related Documentation (Version 7.0)* (Lawrence Livermore National Lab, Oak Ridge, TN).
44. Wolery TJ, Daveler SA (1992) *EQ6, A Computer Program for Reaction Path Modeling of Aqueous Geochemical Systems: Theoretical Manual, User's Guide, and Related Documents* (Lawrence Livermore National Lab, Oak Ridge, TN).